Journal of Fluorine Chemistry 131 (2010) 554–560

Contents lists available at ScienceDirect

Journal of Fluorine Chemistry

journal homepage: www.elsevier.com/locate/fluor

Adsorptive removal of halo-olefinic impurities from 1,1,1,3,3-pentafluoropropane over ion-exchanged Y zeolites

B. Zhang [*], N.F. Shi, C.L. Xu, H.F. Lu, Y.F. Chen, Z.H. Ge

College of Chemical Engineering and Materials Science, Zhejiang University of Technology, 18 Chaowang Road, 310014 Hangzhou, Zhejiang, China

ARTICLE INFO

Article history:
Received 7 September 2009
Received in revised form 28 December 2009
Accepted 29 December 2009
Available online 7 January 2010

Keywords:
Adsorption
Removal
Halo-olefinic impurity
1,1,1,3,3-Pentafluoropropane
Zeolite

ABSTRACT

Various metal cations exchanged Y zeolites were prepared via the exchange of NaY zeolite with aqueous solutions containing K^+, Ca^{2+}, Cu^{2+}, La^{3+} and Ce^{3+} cations, respectively. The influence of the extra-framework cations nature of these ion-exchanged Y zeolites on their adsorption performance for a low content of halo-olefinic impurities, mainly including 1-chloro-3,3,3-trifluoro-1-propene (HCFC-1233zd), 1-chloro-1,3,3,3-tetrafluoro-1-propene (HFC-1224zb) and 2-chloro-1,3,3,3-tetrafluoro-1-propene (HFC-1224xe), in the 1,1,1,3,3-pentafluoropropane (HFC-245fa) product after distillation was investigated. HCFC-1233zd impurity can be substantially removed from HFC-245fa product feed via the adsorption over multivalent metal cations and Cu^+ cation exchanged Y zeolites, which is ascribed to the formation of π-adsorption complexes between HCFC-1233zd and zeolites, rather than over alkaline metal cations exchanged Y zeolites. Among multivalent metal cations exchanged Y zeolites, CeY has the highest adsorption capacity for HCFC-1233zd and best regeneration performance, due to its lowest density of strong Brønsted and weak Lewis acid sites as well as high framework stability during the regeneration. Regardless of the cations introduced in Y zeolite used as an adsorbent, HCFC-1224zb and HCFC-1224xe impurities are not obviously removed from HFC-245fa product feed via the adsorption, maybe due to more halogen atoms linked with the double bond in them comparing with HCFC-1233zd.

1. Introduction

1,1,1,3,3-Pentafluoropropane (HFC-245fa) is a non-ozone depleting compound with an acceptable global warming potential (GWP) [1]. It has been offered recently as a substitute for trichlorofluoromethane (CFC-11), 1,1-dichloro-1-fluoroethane (HCFC-141b) and 1,2-dichloro-1,1,2,2-tetrafluoroethane (CFC-114) [2,3], which are used in a variety of applications including refrigerants, propellants, blowing agents and solvents, and have been perceived as having an adverse effect on the ozone layer and/or as contributing to global warming. In the preparation of HFC-245fa, various halo-olefinic impurities are formed, mainly including 1-chloro-3,3,3-trifluoro-1-propene (HCFC-1233zd), 1,3,3,3-tetrafluoro-1-propene (HFC-1234ze), 1-chloro-1,3,3,3-tetrafluoro-1-propene (HFC-1224zb) and 2-chloro-1,3,3,3-tetrafluoro-1-propene (HFC-1224xe), which must be reduced in concentration to extremely low levels, for example below 0.001 wt%, due to their potential toxicity.

Impurities are generally removed from the desired product by distillation, but this method of removal is made difficult if the boiling point of the impurity is close to that of the desired product. Furthermore, even after distillation, it is possible that small quantities of undesirable impurities will remain. After distillation of the HFC-245fa crude product, halo-olefinic impurities said above will still be present in amounts from about 0.01 to 0.1 wt%, due to the small difference in relative volatility between these unsaturated impurities and HFC-245fa. Thus, there is a need for an alternative purification method to remove residual halo-olefinic impurities from HFC-245fa product sequentially. Many patents have disclosed some methods for the removal of halo-olefins from halo-alkane products through the adsorption on an appropriate adsorbent. For example, the adsorptive separation of vinyl chloride from 1,1-difluoroethane can be performed on an active carbon [4], dichloroacetylene can be substantially removed from a stream of 1,1-dichloro-1-fluoroethane over a carbon molecular sieve having a mean pore size of about 4.2–4.5 Å [5], and the removal of 1-chloro-2,2-difluoroethylene from 1,1,1,2-tetrafluoroethane is accomplished by the adsorption on β- or Y zeolites [6]. However, the removal of a low content of halo-olefinic impurities from HFC-245fa product via the adsorptive separation has not been systematically investigated so far.

For the adsorptive separation of halo-olefinic impurities from HFC-245fa product it is of utmost importance to find a cheap and effective adsorbent. Y zeolite, belonging to the Faujasite type zeolites (FAU), has an open three dimensional pore system with large windows (7.3 Å) that lead to supercages (13 Å), also called α-

---

[*] Corresponding author. Tel.: +86 571 88320417.
E-mail addresses: zb10006093@zjut.edu.cn, zb10006093@tom.com (B. Zhang).

0022-1139/$ – see front matter © 2010 Elsevier B.V. All rights reserved.
doi:10.1016/j.jfluchem.2009.12.021

cages, in which hydrocarbons can adsorb. The negative charges that are introduced into the zeolite framework by $[AlO_4]^{5-}$ building units, are compensated by extra-framework cations. Cations positioned on sites II (SII) and III (SIII) are exposed inside the supercages and are considered to be the most important adsorption sites for alkenes and aromatics [7]. It was reported that in the adsorption of liquid alkene/alkane or aromatic/alkane mixtures, the electrostatic interaction between the double bond and cations introduced in zeolite leads to the selective adsorption of the alkenes and aromatics on NaY compared to alkanes [8]. However, the adsorptive separation of a low content of halo-olefinic impurities from HFC-245fa product using Y zeolite as an adsorbent has not been systematically studied to our knowledge. The adsorption properties of Y zeolite can be substantially modified by altering extra-framework cations. In the work here, the influence of extra-framework cations nature of the ion-exchanged Y zeolites on their adsorption performance for a low content of halo-olefinic impurities in HFC-245fa product after distillation was investigated.

2. Results and discussion

2.1. Materials structure

According to atomic absorption spectroscopy (AAS) analysis, the KY, CaY, CuY, LaY and CeY zeolites with ion exchange degrees of 96.4%, 90.1%, 87.2%, 93.3% and 95.4% relative to complete sodium-other cation substitution in the zeolite, respectively, were obtained. A change in color of CuY from blue to green during the calcination stage suggests that Cu^{2+} cations are reduced to Cu^{+} cations [9].

Fig. 1 shows the XRD patterns of NaY and ion-exchanged Y zeolites. The XRD pattern of NaY is identical to those reported in the literature [10,11], and after ion exchange with K^+, Ca^{2+}, Cu^{2+}, La^{3+} and Ce^{3+} cations, respectively, the XRD patterns of ion-exchanged Y zeolites maintain the original crystalline structure. The above patterns including the absence of a distinct broad reflection between 20° and 25° (2θ), which would indicate the presence of amorphous silica, demonstrate that the FAU structure remains intact after each ion exchange. Some decrease in the intensity of the reflections observed in the XRD patterns of LaY and CeY materials may be attributed to an enhanced adsorption of X-rays in the presence of the rare-earth cations, rather than to a decreased crystallinity, and can be taken as an indication for the successful ion exchange [10].

Fig. 2 presents the infrared spectra in the structural region for NaY and ion-exchanged Y zeolites. As previously published [12], ion exchange with K^+, Ca^{2+}, Cu^{2+}, La^{3+} or Ce^{3+} cations does not bring about significant changes in the structural region of Y zeolites, since interactions between the extra-framework cations and the zeolite framework are generally weak, also indicating that the FAU structure remains basically intact after each ion exchange. Nevertheless, some small differences in the spectra are observed. The bands at 950–1250 cm^{-1} attributed to the asymmetric stretching of the tetrahedral TQ_4 are shifted to higher wavenumbers as sodium is exchanged by multivalent cations. In addition, the band at 578 cm^{-1}, assigned to external bonds of the double six rings, becomes less intense as the exchange of Na^+ with Ca^{2+} and Ce^{3+} cations respectively, takes place. Such intensity reduction is normally an indication of crystallinity loss, however, it has also been interpreted as a consequence of cation migration from the sodalite cage to the center of the double six ring [12].

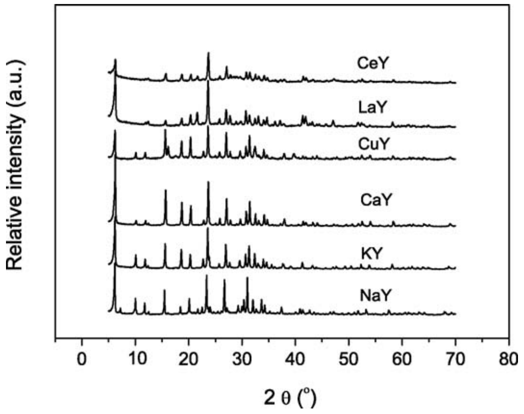

Fig. 1. XRD patterns of NaY and ion-exchanged Y zeolites.

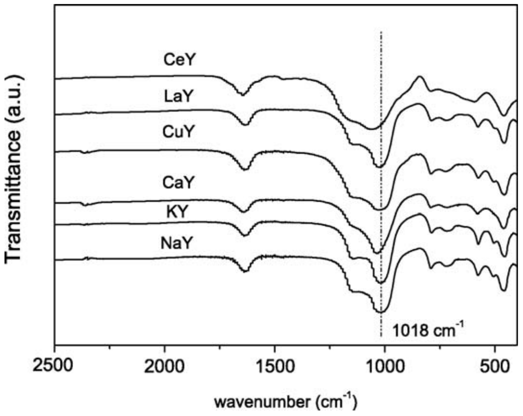

Fig. 2. FTIR spectra of NaY and ion-exchanged Y zeolites.

2.2. Influence of the extra-framework cations nature of the ion-exchanged Y zeolites on their adsorption for halo-olefins

Fig. 3A–D depicts the contents of HCFC-1233zd, HCFC-1224zb and HCFC-1224xe as well as HFC-245fa in the effluent after the adsorption of HFC-245fa product feed over NaY, KY, CaY, CuY, LaY and CeY zeolites respectively, as a function of the temperature from 303 to 453 K. For HCFC-1233zd, the usage of NaY and KY zeolites as adsorbents did not lead to a visible decrease of its content in the effluent comparing with that in HFC-245fa product feed (listed in Table 1) at the whole temperature range. However, after the adsorption on the CaY, CuY, LaY or CeY zeolites, the content of HCFC-1233zd in the effluent dropped to under 0.001 wt% at the temperature ranges from 363 to 453 K. Contrary to HCFC-1233zd, at the whole adsorption temperature range investigated, the contents of HCFC-1224zb and HCFC-1224xe in the effluent were like to those in HFC-245fa product feed, after the adsorption over the six kinds of ion-exchanged Y zeolites. In order to eliminate the influence of a hypothetically competitive adsorption between HCFC-1233zd and HCFC-1224zb or HCFC-1224xe on the adsorption behaviors of HCFC-1224zb and HCFC-1224xe on these ion-exchanged Y zeolites, we also carried out the adsorption experiments for HFC-245fa product only containing HCFC-1224zb and HCFC-1224xe halo-olefins, from which HCFC-1233zd had been almost completely removed by adsorption, over CaY, CuY and CeY zeolites respectively, at the same temperature range. Almost no decrease of the contents of HCFC-1224zb and HCFC-1224xe in the effluent was observed comparing with HFC-245fa product feed.

An obvious influence of adsorption temperature on the adsorption behavior of HCFC-1233zd on CaY, CuY, LaY and CeY zeolites was observed. The relatively low adsorption temperature (333 K) could result in a deterioration of adsorption of HCFC-1233zd, indicated by an increase of content of HCFC-1233zd in the

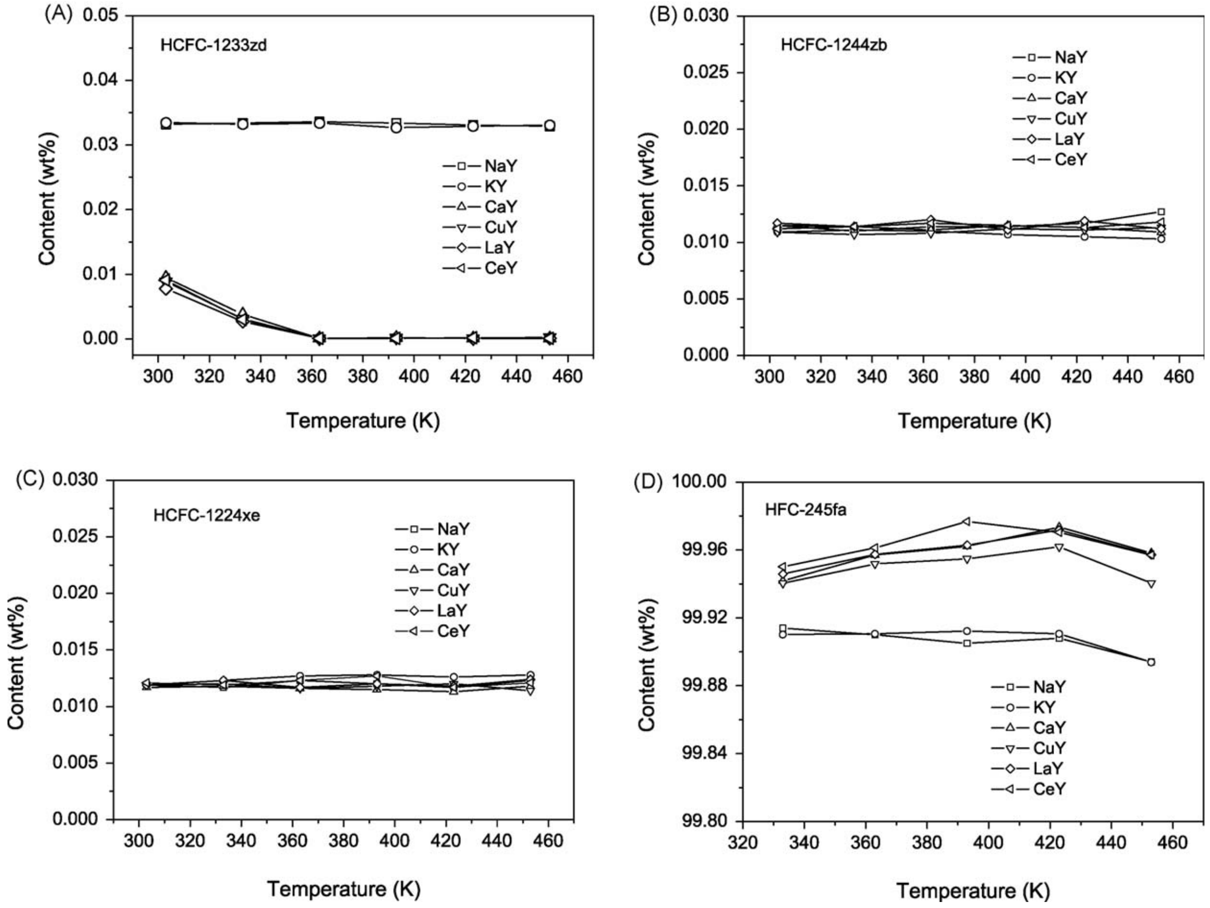

Fig. 3. Adsorption of NaY and ion-exchanged Y zeolites for HCFC-1233zd (A), HCFC-1224zb (B), HCFC-1224xe (C) and HFC-245fa (D) at different temperatures.

effluent, about 0.009 wt%. But the relatively high temperature (453 K) could lead to a drop of the content of HFC-245fa (below 0.03 wt%), along with an appearance of HFC-1234ze (1,3,3,3-tetrafluoro-1-propene, about 0.026, 0.013, 0.003, 0.015, 0.003, 0.003 wt% for NaY, KY, CaY, CuY, LaY and CeY, respectively) in the effluent.

Briefly, the adsorption of HCFC-1233zd from HFC-245fa product feed over these various cations exchanged Y zeolites is strongly dependent on the extra-framework cations nature. HCFC-1233zd can be substantially removed from HFC-245fa product feed by the adsorption over CaY, LaY, and CeY zeolites which contain multivalent cations and CuY zeolite which contains univalent cation Cu^+, rather than over NaY and KY zeolites which contain univalent alkaline metal cations. Inversely, regardless of the cations incorporated in Y zeolite using as an adsorbent, HCFC-1224zb and HCFC-1224xe cannot be obviously removed from HFC-245fa product feed via the adsorption.

Generally it is observed that alkenes are preferentially adsorbed from their mixture with alkane solvents on Faujasite type zeolites containing univalent extra-framework cations such as Na^+ and K^+, as a result of the specific interaction of the π-electrons of the double bond with the electrostatic field gradient of the cations incorporating in zeolites [7,8]. The adsorption of alkanes on zeolite is simply physisorption corresponding to the van der Waals interactions between the alkanes and the zeolite surface. The higher the dipole moment of molecular is, the stronger the strength of the van der Waals interaction is [13,14]. However, in the present study, all of HFC-1233zd, HCFC-1224zb and HCFC-1224xe cannot be effectively adsorbed from HFC-245fa product feed on NaY and KY zeolites. This behavior can be explained in terms of the significant stronger electronegativity of halogen atoms containing in these halo-olefins and HFC-245fa comparing with hydrogen atom, which leads to a distinct decrease of π-electron density of the double bond and a marked increase of dipole moment for these halo-olefins and HFC-245fa molecules. Therefore the adsorbate–adsorbent interactions of both halo-olefinic impurities and HFC-245fa with NaY or KY are mainly governed by the van der Waals interaction, consequently resulting in no significant difference in adsorption affinity between these halo-olefins and HFC-245fa [15,16]. Contrary to NaY and KY zeolites, after the adsorption on CuY zeolite which also contains univalent cation Cu^+, HCFC-1233zd is almost completely removed from HFC-245fa product feed at a certain temperature range. It can be explained by that the double bond of HCFC-1233zd can form π-complexes with Cu^+ cations in the CuY zeolite through the donation of π-electrons of the halo-olefin to the empty σ-orbital of Cu^+ and the backdonation of d-electrons of Cu^+ to the π*-orbital of the halo-olefin. It has been reported that the double bond of the olefin can form π-complexes with some transition metal cations such as Cu^+ and Ag^+, and a difference in adsorption affinity between olefin and alkane can be achieved [17,18]. HCFC-1233zd can also

Table 1
The contents of halo-olefins and HFC-245fa[a] in HFC-245fa[a] product after distillation.

Component	HFC-245fa[a]	HCFC-1233zd[b]	HCFC-1224zb[c]	HCFC-1224xe[d]
Content (wt%)	99.913	0.034	0.011	0.012

[a] HFC-245fa: 1,1,1,3,3-pentafluoropropane.
[b] HCFC-1233zd: 1-chloro-3,3,3-trifluoro-1-propene.
[c] HCFC-1224zb: 1-chloro-1,3,3,3-tetrafluoro-1-propene.
[d] HCFC-1224xe: 2-chloro-1,3,3,3-tetrafluoro-1-propene.

be nearly completely removed from HFC-245fa product feed over CaY, LaY and CeY zeolites which contain multivalent cations Ca^{2+}, La^{3+} and Ce^{3+}, respectively. Numerous researches concerning zeolites-catalyzed hydrocarbon transformations, such as cracking, isomerization and alkylation, show that alkene molecules can be adsorbed on the Brønsted acid sites of zeolites via π-adsorption complexes, that is, covalent alkoxide species, where the π-electron of the double bond forms a hydrogen bonding with the Brønsted acidic proton of the zeolite, as the most stable adsorbed structure [13,15,16,19,20]. It is well known that Brønsted acid sites are generated via the hydrolysis of water molecules associated to the multivalent metal cations in the zeolite [12,21]. In this work, after most of Na^+ in the Y zeolite undergoes exchange by Ca^{2+}, La^{3+} and Ce^{3+} respectively, and subsequent calcination, the Brønsted acid sites arise in CaY, LaY and CeY zeolites. Therefore the adsorption of CaY, LaY and CeY zeolites for HCFC-1233zd from HFC-245fa product feed is mainly ascribed to the formation of π-adsorption complexes of HCFC-1233zd with the Brønsted acid sites in these zeolites. Similar π-adsorption complexes of HCFC-1233zd cannot form in NaY and KY zeolites, due to the absence of Brønsted acid sites in them [12,22,23]. In a word, the adsorption of HCFC-1233zd on these various cations exchanged Y zeolites is mainly dependent on the formation of π-adsorption complexes between the halo-olefin and zeolites.

Contrary to HCFC-1233zd, HCFC-1224zb and HCFC-1224xe can be hardly removed from R245fa product feed via the adsorption over CaY, CuY, LaY and CeY zeolites. This phenomena may be attributed to the more halogen atoms linked with the double bond in HCFC-1224zb and HCFC-1224xe molecules than in HCFC-1233zd molecule (two halogen atoms vs. one halogen atom), which results in the too low density of π-electrons of the double bond and stronger steric hindrance of bulky halogen atoms during the interaction with the Brønsted acid sites or Cu^+ cations.

In many studies on the activation of alkanes over acidic zeolite catalysts, it has been reported that alkanes can also be activated by the Brønsted or Lewis acid sites in zeolites to give unstable transition states known as carbonium ions or covalent alkoxide species, subsequently, to undergo cracking to yield olefins, at the higher temperature comparing to alkenes [20,24]. It has been also proposed that, in presence of alkyl halides, the zeolitic oxygen can act as a base by abstracting the β-proton, while the framework cation stabilizes the halogen, resulting in the olefin formation [25,26]. It has also been reported that, in the presence of Lewis acids such as the metal oxides and metal fluorides, the elimination of HF from HFC-245fa occurs easily at high temperature [2]. Hess and Kemnitz found that the principal product of the dehydrochlorination reaction of CH_3CCl_3 on fluorinated γ-alumina containing Lewis as well as Brønsted acid sites, which is mostly favored thermodynamically above 423 K, was $CH_2{=}CCl_2$ [27]. Thus, in this work, a slight drop of HFC-245fa, below 0.03 wt%, in the effluent after the adsorption on the NaY, KY, CuY, CaY, LaY and CeY zeolites at 453 K can be ascribed to the catalytic elimination of HF from HFC-245fa, verified by the appearance of a few amount of HFC-1234ze, below 0.03 wt%, in the effluent at 453 K.

The adsorption of HCFC-1233zd on CaY, CuY, LaY and CeY zeolites is chemisorption, which needs some adsorption activation energy, verified by that HCFC-1233zd could be almost completely removed from R245fa product feed over these zeolites only when the adsorption temperature exceeded 363 K.

2.3. Breakthrough experiments

The breakthrough experiments were performed for HCFC-1233zd. Fig. 4 represents the breakthrough profiles of HCFC-1233zd (0.034 wt%) in the HFC-245fa product feed at 363 K and a WHSV (weight-hourly space velocity) of 0.5 h^{-1} through a 10 cm column packed with 5 g of CuY, CaY, LaY and CeY zeolites, respectively. From the breakthrough profile the amount of adsorbed HCFC-1233zd (q, mg g^{-1}) was calculated using the following formula (1):

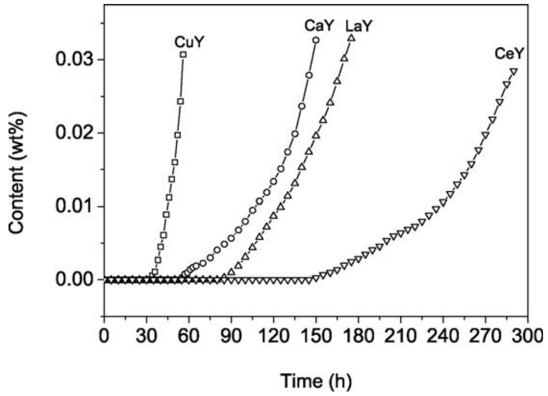

Fig. 4. Breakthrough profiles of HCFC-1233zd (0.034 wt%) in HFC-245fa feed at 363 K on columns packed with CuY, CaY, LaY and CeY zeolites respectively.

$$q = \int_0^t u \times (C_{\text{in}} - C_{\text{out}})dt \qquad (1)$$

with u the weight flow rate of the HFC-245fa product feed (g h^{-1}), C_{in} and C_{out} the concentration (wt%) of HCFC-1233zd in the HFC-245fa product feed and effluent, respectively.

Practically from the beginning of the experiment, HFC-245fa product free of HCFC-1233zd after the adsorption over CuY, CaY, LaY and CeY was obtained until about 33.2, 55.1, 84.8, 149.9 h on stream, respectively. Using formula (1), the amounts of HCFC-1233zd adsorbed on the CuY, CaY, LaY and CeY before the breakthrough were calculated to be 5.4, 9.2, 13.4, 24.6 mg g^{-1} respectively. The adsorption capacity of the four ion-exchanged Y zeolites for HCFC-1233zd decreases in the order of CeY > LaY > CaY > CuY.

The oligomerization of light olefins over acidic catalysts is a well known reaction [28,29]. For example, the trimerization of isobutene can be carried out over ferrite [30], dealuminated Y [31] or beta zeolites [32], and similarly, propene is oligomerized to C_6, C_9, etc., over ZSM-5 [33] or HY [34] zeolites at low temperature, where the addition species of isobutene or propene on acid sites in these catalysts act as chain carriers [30–34]. As such, it is plausible that the oligomerization reaction of HCFC-1233zd may take place over CaY, LaY or CeY zeolites and the oligomers may be retained by the zeolite framework [13,35] at a low temperature of 363 K and under a low WHSV of HFC-245fa product feed, such as 0.5 h^{-1}, in this work. The adsorption capacities of CaY, LaY and CeY zeolites for HCFC-1233zd may be associated with the oligomerization reaction of HCFC-1233zd on them. The suitable degree of oligomerization may favor an increase of the amount of HCFC-1233zd adsorbed on these ion-exchanged Y zeolites. However, with a higher degree of oligomerization, it is possible that the chain growth of polyolefinic species which lead toward heavier oligomerization products, for example, coke precursors or cokes, is sufficient to gradually block the channel in these zeolites, which limits the access of HCFC-1233zd to the Brønsted acid sites and thus leads to an important drop of the adsorption capacities of these zeolites for HCFC-1233zd. The black external surface of a considerable part of spent CaY zeolite grains suggests the formation of coke in them during the adsorption. The degree of oligomerization of light olefins over acidic Y zeolites is related to the strength and density of acid sites. The stronger strength and higher density of acid sites may lead to the formation of heavier oligomerization products [36,37]. The acidic properties of the CaY,

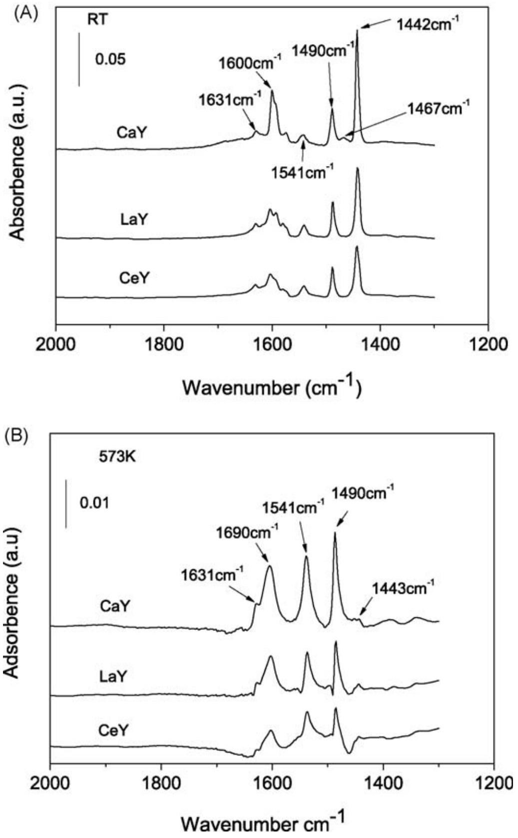

Fig. 5. Pyridine-FTIR spectra of CaY, LaY and CeY after desorption at room temperature (A) and 573 K (B).

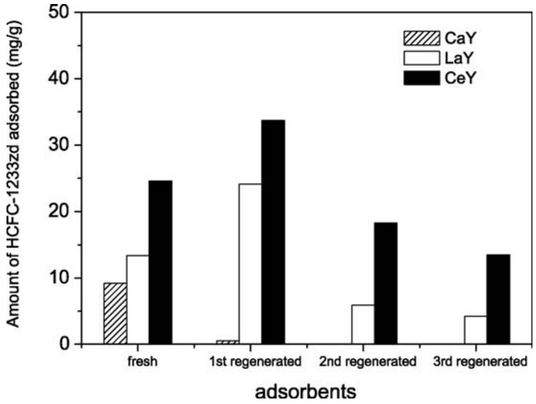

Fig. 6. Amount of HCFC-1233zd adsorbed on fresh and regenerated adsorbents.

LaY and CeY zeolites were studied by pyridine adsorption followed by infrared spectroscopy. Infrared spectra of pyridine after desorption at room temperature in the range 1400–2000 cm^{-1} are shown in Fig. 5A for CaY, LaY and CeY zeolites. Pyridine adsorbed on the three samples results in the appearance of bands around 1541 and 1631 cm^{-1} attributed to pyridine adsorbed on Brønsted acid sites, the band at 1490 cm^{-1} assigned to pyridine adsorbed on both Brønsted and Lewis acid sites, as well as the bands at 1600 and 1442 cm^{-1} attributed to pyridine bonded to multivalent metal cations (M^{n+}) and related to M–O–Al linkages originating new Lewis acid sites [38]. In CaY, an additional weak band is also detected at 1457 cm^{-1} which is hardly visible in LaY and CeY. It may be ascribed to pyridine adsorbed to Lewis acid sites [12,38,39]. For the three samples, the intensity of bands corresponding to new Lewis acid sites increases in the order of CeY < LaY < CaY and the intensity of bands assigned to Brønsted acid sites is similar. Fig. 5B shows the infrared spectra of pyridine after desorption at 573 K for CaY, LaY and CeY. All samples are able to retain pyridine bonded to Brønsted acid sites after desorption at 573 K while the band characteristics of new Lewis acid sites nearly disappear, which reveals the presence of strong Brønsted and weak Lewis acid sites in the three samples. The intensity of bands at 1541 and 1631 cm^{-1} after desorption at 573 K decreases in the sequence: CaY > LaY > CeY. These results show that CaY has the highest density of weak Lewis and strong Brønsted acid sites, followed by LaY, CeY. Thus, it is estimated that the order of an occurrence of cannel blocking due to the formation of heavier oligomerization products is as follows: CaY > LaY > CeY. This estimation is agreed with a change in color of a part of CaY and LaY zeolites grains from white to black and to slight yellow, respectively, as well as almost no change in color of CeY zeolite grains during the adsorption, which suggests that the coke formation degree in the three zeolites during the adsorption decreased in the order of CaY > LaY > CeY. Therefore, the amount of HCFC-1233zd adsorbed on these samples increases in the order of CaY < LaY < CeY.

The π-complexes formed via the interaction of HCFC-1233zd with Cu^+ cations in CuY zeolite may not undergo oligomerization reaction, i.e., one Cu^+ site may only adsorb a molecule of HCFC-1233zd. Hence, the amount of HCFC-1233zd adsorbed on CuY is significant lower than those on CaY, LaY and CeY.

2.4. Adsorbent regeneration

The regeneration performance of an adsorbent plays a key role in its actual applications. In this study, the spent CaY, LaY and CeY were selected to be regenerated at 573 K for 10 h under a nitrogen flow of 30 mL min^{-1}. Breakthrough experiments for HCFC-1233zd in HFC-245fa product feed at 363 K were carried out for these regenerated adsorbents again, in which the amounts of adsorbed HCFC-1233zd before the breakthrough were also calculated, according to the formula (1), and shown in Fig. 6, along with the amounts of HCFC-1233zd adsorbed on the fresh adsorbents. One may notice that, comparing the amounts of HCFC-1233zd adsorbed on the first regenerated adsorbents to those on fresh adsorbents, the 1.8-fold and 1.4-fold increases as well as an approximately 18.4-fold reduction were observed for LaY, CeY and CaY, respectively. Although the amounts of HFC-1233zd adsorbed on LaY and CeY gradually decreased upon the subsequent regenerations, it on the third regenerated CeY was still higher than that on the fresh CaY and exceeded a half of that on the fresh CeY. The above results indicate that the regeneration performance of LaY and CeY zeolites is superior to that of CaY zeolite.

These results can be explained by two reasons. One is possibly that, comparing with the heavier oligomerization products of HCFC-1233zd on CaY, those on LaY and CeY may be easily desorbed from the adsorbents during the regeneration, subsequently leading to the easier restoration of adsorptive active sites. The other is related to the framework stability of the three ion-exchanged Y zeolites during the regeneration. The XRD patterns of the first regenerated CaY as well as the third regenerated LaY and CeY zeolites are seen in Fig. 7, in which those of the fresh CaY, LaY and CeY zeolites are also included. Compared to the fresh CaY, a distinct decrease in the intensity of the reflections can be observed in the XRD pattern of the first regenerated CaY. On the other hand, the XRD patterns of fresh as well as the third regenerated CeY and LaY are similar. The XRD results indicate that the regeneration led to a severe damage to the crystal structure of CaY while did not obviously affect the crystal structure of CeY and LaY. The changes between the XRD patterns of fresh and regenerated ion-exchanged Y zeolites found in Fig. 7 strongly suggest that the framework

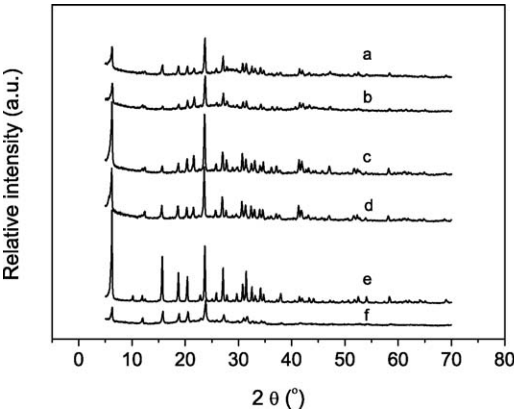

Fig. 7. XRD patterns of the fresh and the third regenerated CeY (a and b), LaY (c and d), as well as the fresh and the first regenerated CaY (e and f).

stability of ion-exchanged Y zeolites during the regeneration plays a significant role in the regeneration performance of them. The destruction of the framework of ion-exchanged Y zeolites may result in a significant change of the location as well as the density and strength of acid sites in them and thus a dramatic deterioration of their adsorption ability for HCFC-1233zd. During the regeneration the decomposition of the adsorbed oligomerization products could take place to generate the HF and/or HCl, indicated by the acidity (a pH value of ca. 3.0 measured by a pH indicator paper) of the regeneration gas coming from the regeneration fixed bed outlet, and an appearance of white opaque in the aqueous solution adsorbing the outlet regeneration gas by adding 0.1 M $AgNO_3$ solution in it. The HF and HCl might react with the aluminium and silicon atoms in the zeolite framework, leading to a transformation of some framework aluminium and silicon atoms to extra-framework octahedral aluminium and silicon species and then a gradual destruction of the zeolite framework, indicated by an important reduction of the intensity of the reflections in the XRD pattern of the regenerated CaY. Because of the formation of coordination bonds between rare-earth metal cations and the framework oxygen atoms in the zeolites that stabilizes the sodalite units [40–42], rare-earth metal cations La^{3+} and Ce^{3+} in LaY and CeY zeolites might effectively prevent the destruction of their framework, thus resulting in their high framework stability during the regeneration, which in turn led to their better adsorption regeneration performance for HCFC-1233zd comparing with CaY zeolite.

We speculate that the higher amounts of HCFC-1233zd adsorbed on the first regenerated LaY and CeY zeolites than those on the fresh LaY and CeY zeolites are related to the variation of acid properties in the two zeolites upon the first regeneration, but further studies are required to test this hypothesis. The amounts of HCFC-1233zd adsorbed on the regenerated LaY and CeY zeolites decreased in the order of the first regeneration > the second regeneration > the third regeneration, as expected, due to a gradual increase of residual carbonaceous deposits formed from the oligomers on the acid sites in the spent adsorbents which resulted in a gradual decrease of amount of adsorption active sites [40,43].

3. Conclusions

HCFC-1233zd impurity can be substantially removed from HFC-245fa product after distillation via the adsorption over Ca^{2+}, La^{3+} and Ce^{3+} multivalent metal cations as well as Cu^{+} cation exchanged Y zeolites rather than over Na^{+} and K^{+} alkaline metal cations exchanged Y zeolites. The adsorption of HCFC-1233zd on various metal cations exchanged Y zeolites may be dependent on the formation of π-adsorption complexes between it and zeolites. Regardless of the cations introduced in Y zeolite using as an adsorbent, HCFC-1224zb and HCFC-1224xe impurities are hardly removed from HFC-245fa product feed via the adsorption, maybe due to the more halogen atoms linked with the double bond in them comparing with HCFC-1233zd. For CaY, LaY and CeY zeolites, not only the adsorption capacity for HCFC-1233zd but also the regeneration performance increase in the order of CaY < LaY < CeY. For the three samples, FTIR results of adsorbed pyridine suggest that the lower density of strong Brønsted and weak Lewis acid sites may be favorable to the increase in adsorption capacity of them for HCFC-1233zd. The comparing XRD results between fresh and regenerated ion-exchanged Y zeolites show that the higher framework stability of a Y zeolite during the regeneration may lead to its better regeneration performance.

4. Experimental

4.1. Materials preparation

The ion-exchanged Y zeolites in this study were prepared from NaY zeolite (Si/Al = 2.68) obtained from Henye chemical plant (Shanghai, China). The $CaCl_2$ (≥96.0%), KCl (≥99.0%), $Cu(NO_3)_2\cdot 3H_2O$ (≥99.0%), $La(NO_3)\cdot 6H_2O$ (≥98.0%), $Ce(NO_3)\cdot 6H_2O$(≥98.0%), analytically pure, were purchased from China Medicine (group) Huadong Chemical Reagent Corp (Hangzhou, China). All of chemicals were used as received without further purification. All ion-exchanged Y zeolites were prepared following the same ion exchange procedure. For example, to achieve Ca-exchanged Y zeolite (CaY), the NaY zeolite was ion exchanged with a 0.2 M calcium chloride solution at 353 K for 2 h using a ratio of solution to zeolite of 10 mL g^{-1}, followed by washing with bi-distilled water for several times. Then the sample was dried at 383 K and calcined at 773 K for 3 h in air. This procedure repeated twice more, resulting in the attainment of a higher level of exchange of Na^{+} with Ca^{2+}.

4.2. Characterization of materials

The NaY and ion-exchanged Y zeolites were characterized by X-ray diffraction (XRD), using a Rigaku diffractometer with Cu Kα radiation. Infrared spectra of samples were recorded on a Nicolet 370 FTIR spectrophotometer from KBr wafers containing 1 wt% of the sample. The contents of cations in the ion-exchanged Y zeolites were determined by atomic absorption spectroscopy (AAS).

FTIR spectra of pyridine adsorbed on CaY, LaY and CeY zeolites were obtained using a Nicolet Nexus FTIR spectrometer. The zeolites were pelletized to wafers and evacuated for 4 h at 573 K, then cooled to ambient temperature under vacuum (~10^{-5} Torr). After recording the initial spectrum of the sample at ambient temperature (reference), pyridine was adsorbed at ambient temperature for 30 min under an equilibrium pressure of 2.7 mbar. The spectra were recorded at ambient temperature after degassing the sample for 1 h, at the required temperature (423–573 K) and using a heating rate of 5 K min^{-1}. The background spectrum, recorded under identical operating conditions without sample, was always performed before each spectrum and automatically subtracted. The spectra of pyridine adsorbed on the sample were corrected by subtracting the reference spectrum from them. Band intensities were normalized by the sample weight.

4.3. Adsorption experiment

The main halo-olefins impurities contained in the HFC-245fa product after distillation, kindly provided by Zhejiang Lantian

Environmental Protection Hi-Tech Co., Ltd. (Hangzhou, China), are HCFC-1233zd, HCFC-1224zb and HCFC-1224xe, and the contents of which and HFC-245fa are listed in Table 1.

Adsorption experiments of HFC-245fa product feed said above on NaY and ion-exchanged Y zeolites were performed in gas phase using a fixed bed continuous flow reactor (10 mm i.d.) with a thermocouple in the center of the adsorbent bed, at 333–453 K and atmospheric pressure. 5.0 g of adsorbent (30–40 mesh) was loaded into the adsorbent bed. Prior to the feeding, HFC-245fa product was gasified at 323 K, and it without dilution was used as the feed. The adsorbent was pre-treated in situ at 573 K for 5 h under a nitrogen flow of 30 mL min^{-1} before starting an adsorption run. Then HFC-245fa product feed was passed through the adsorbent bed at the desired temperature. The space velocity of HFC-245fa product feed, WHSV (weight-hourly space velocity, g of HFC-245fa product feed per g of adsorbent per hour), was maintained at 0.5 h^{-1} by controlling the flow rate of HFC-245fa product feed. After running of 30 min, the concentrations of components in the effluents were analyzed on an Agilent 6890N gas chromatograph equipped with a FID and a DB1301 column.

Breakthrough experiments were also performed in a fix-bed reactor under the experimental conditions described above except for a fixed adsorption temperature of 363 K.

When one adsorption bed reached a saturated adsorption, the regeneration of the spent zeolite was performed in situ at 573 K for 10 h under a nitrogen flow of 30 mL min^{-1}. Then breakthrough experiments were carried out for the regenerated adsorbents under the experimental conditions said above again.

Acknowledgements

The authors want to gratefully thank Science and Technology Department of Zhejiang Province (Project No. 2007C11043) and Zhejiang Lantian Environmental Protection Hi-Tech Co., Ltd for the financial support to this research.

References

[1] IPCC 3rd Report, Climate Change 2001 (the Scientific Basis), 2001, p. 388.
[2] H.D. Quan, H.E. Yang, M. Tamura, A. Sekiya, J. Fluorine Chem. 128 (2007) 190–195.
[3] V.P. Zhelezny, Y.V. Semenyuk, S.N. Ancherbak, A.J. Grebenkov, O.V. Beliayeva, J. Fluorine Chem. 128 (2007) 1029–1038.
[4] P. Pascal, US Patent 5,396,001 (1995).
[5] Y.F. Stephen, US Patent 4,940,825 (1990).
[6] C. Stuart, M.J. Charles, US Patent 7,084,315 (2006).
[7] I. Daems, P. Leflaive, A. Méthivier, J.F.M. Denayer, G.V. Baron, Micropor. Mesopor. Mater. 82 (2005) 191–199.
[8] I. Daems, P. Leflaive, A. Méthivier, G.V. Baron, J.F.M. Denayer, Micropor. Mesopor. Mater. 96 (2006) 149–156.
[9] A. Anson, Y. Wang, C.C.H. Lin, T.M. Kuznicki, S.M. Kuznicki, Chem. Eng. Sci. 63 (2008) 4171–4175.
[10] E.L. Pires, J.C. Magalhães, U. Schuchardt, Appl. Catal. A: Gen. 203 (2000) 231–237.
[11] C.R. Moreira, M.M. Pereira, X. Alcobé, N. Homa, J. Llorca, J.L.G. Fierro, P.R. Piscina, Micropor. Mesopor. Mater. 100 (2007) 276–286.
[12] E.F.S. Aguiar, V.L.D. Camorim, F.M.Z. Zotin, R.L.C. Santos, Micropor. Mesopor. Mater. 25 (1998) 25–34.
[13] G. Onyestyák, L.V.C. Rees, Appl. Catal. A: Gen. 223 (2002) 57–64.
[14] D.M. Ruthven, S.C. Reyes, Micropor. Mesopor. Mater. 104 (2007) 59–66.
[15] P. Pantu, B. Boekfa, J. Limtrakul, J. Mol. Catal. A: Chem. 277 (2007) 171–179.
[16] A. Corma, F.J. Ortega, J. Catal. 233 (2005) 257–265.
[17] J.F.M. Denayer, A. Deola, W. Vermandel, F. Gemoets, F.V. Buren, J. Martens, C. Kirschhock, G.V. Baron, P.A. Jacobs, Micropor. Mesopor. Mater. 103 (2007) 11–19.
[18] A.V. Miltenburg, W. Zhu, F. Kapteijn, J.A. Moulijn, Chem. Eng. Res. Des. 84 (2006) 350–354.
[19] J. Limtrakul, T. Nanok, S. Jungsuttiwong, P. Khongpracha, T.N. Truong, Chem. Phys. Lett. 349 (2001) 161–166.
[20] G. Caeiro, R.H. Carvalho, X. Wang, M.A.N.D.A. Lemos, F. Lemos, M. Guisnet, F.R. Ribeiro, J. Mol. Catal. A: Chem. 255 (2006) 131–158.
[21] T. Noda, K. Suzuki, N. Katada, M. Niwa, J. Catal. 259 (2008) 203–210.
[22] R.C. Deka, K. Hirao, J. Mol. Catal. A: Chem. 181 (2002) 275–282.
[23] G. Martra, R. Ocule, L. Marchese, G. Centi, S. Coluccia, Catal. Today 73 (2002) 83–93.
[24] C.H. Liu, X.H. Gao, Z.D. Zhang, H.T. Zhang, S.H. Sun, Y.Q. Deng, Appl. Catal. A: Gen. 264 (2004) 225–228.
[25] C.W. Kanyi, D.C. Doetschman, J.T. Schulte, K. Yan, R.E. Wilson, B.R. Jones, C.O. Kowenje, S.W. Yang, Micropor. Mesopor. Mater. 92 (2006) 292–299.
[26] C.W. Kanyi, D.C. Doetschman, S.W. Yang, J. Schulte, B.R. Jone, Micropor. Mesopor. Mater. 108 (2008) 103–111.
[27] A. Hess, E. Kemnitz, J. Fluorine Chem. 74 (1995) 27–35.
[28] K. Hauge, E. Bergene, D. Chen, G.R. Fredriksen, A. Holmen, Catal. Today 100 (2005) 463–466.
[29] H.Q. Zhou, Y. Wang, F. Wei, D.Z. Wang, Z.W. Wang, Appl. Catal. A: Gen. 348 (2008) 135–141.
[30] J.W. Yoon, J.H. Lee, J.S. Chang, D.H. Choo, S.J. Lee, S.H. Jhung, Catal. Commun. 8 (2007) 967–970.
[31] J.W. Yoon, S.H. Jhung, D.H. Choo, S.J. Lee, K.Y. Lee, J.S. Chang, Appl. Catal. A: Gen. 337 (2008) 73–77.
[32] J.W. Yoon, J.S. Chang, H.D. Lee, T.J. Kim, S.H. Jhung, J. Catal. 245 (2007) 253–256.
[33] R.J. Quann, L.A. Green, S.A. Tabak, F.J. Krambeck, Ind. Eng. Chem. Rev. 27 (1988) 565–570.
[34] J.F. Haw, B.R. Richardson, I.S. Oshiro, N.D. Lazo, J.A. Speed, J. Am. Chem. Soc. 111 (1989) 2052–2058.
[35] A.G. Stepanov, M.V. Luzgin, V.N. Romannikov, V.N. Sideinikov, E.A. Paukahtis, J. Catal. 178 (1998) 466–477.
[36] B. Nkosi, F.T.T. Ng, G.L. Rempel, Appl. Catal. A: Gen. 161 (1997) 153–166.
[37] F.A.D. Mendoza, L.P. Bolaño, N.C. Martño, N.C. Martínez, Thermochim. Acta 312 (1998) 47–61.
[38] A. Martins, J.M. Silva, C. Henriques, F.R. Ribeiro, M.F. Ribeiro, Catal. Today 107–108 (2005) 663–670.
[39] Z.K. Zhao, W.H. Qiao, X.N. Wang, G.R. Wang, Z.S. Li, L.B. Cheng, Micropor. Mesopor. Mater. 94 (2006) 105–112.
[40] H.S. Cerqueira, G. Caeiro, L. Costa, F.R. Ribeiro, J. Mol. Catal. A: Chem. 292 (2008) 1–13.
[41] M.A.S. Castillo, R.J. Madon, J.A. Dumesic, J. Phys. Chem. B 109 (2005) 2164–2175.
[42] M.L. Occelli, P. Ritz, Appl. Catal. A: Gen. 183 (1999) 53–59.
[43] A.S. Escobar, M.M. Pereira, H.S. Cerqueira, Appl. Catal. A: Gen. 339 (2008) 61–67.